Fire resistance of double-skinned composite tubular columns including concrete confinement

Deok Hee Won, Taek Hee Han, Seungjun Kim & Young Jong Kang

Materials and Structures

ISSN 1359-5997

Mater Struct
DOI 10.1617/s11527-015-0575-9

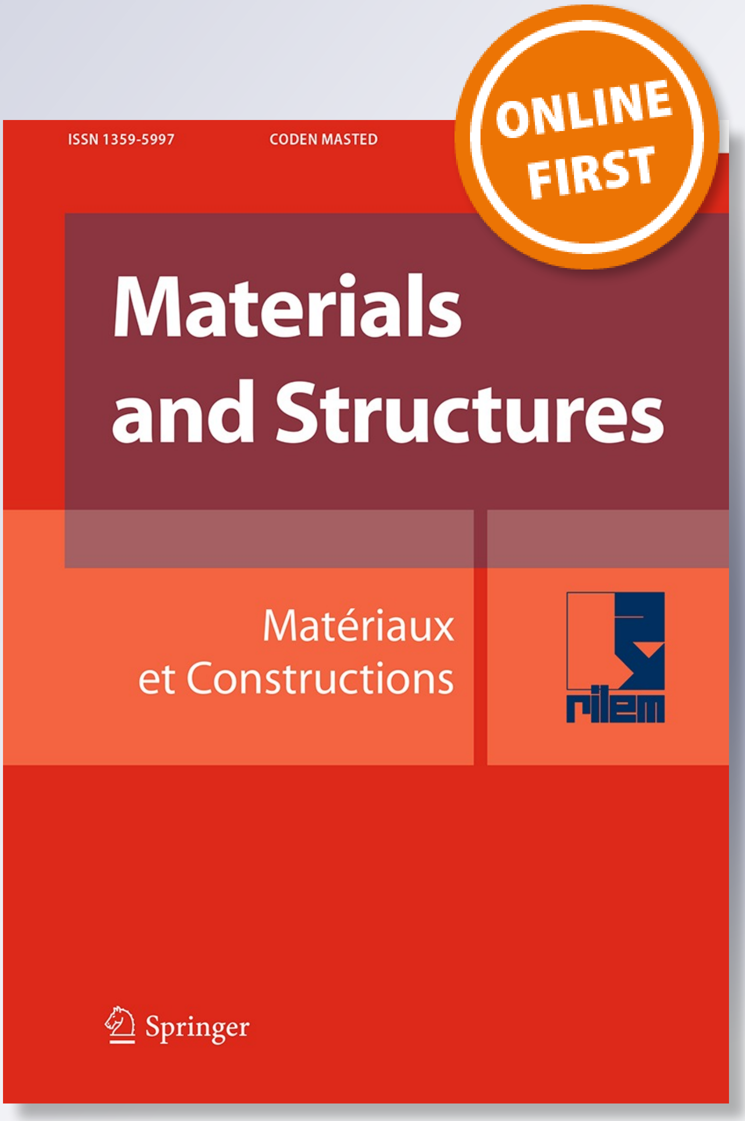

Springer

Materials and Structures
DOI 10.1617/s11527-015-0575-9

ORIGINAL ARTICLE

Fire resistance of double-skinned composite tubular columns including concrete confinement

Deok Hee Won · Taek Hee Han · Seungjun Kim · Young Jong Kang

Received: 7 October 2014 / Accepted: 22 February 2015

Abstract Double-skinned composite tubular (DSCT) columns consisting of concrete cast between outer and inner tubes have been developed to overcome certain limitations of other columns, such as the large self-weight of concrete-filled tubular columns and lack of concrete confinement of hollow concrete-filled tubular columns. The strength and ductility of the column are enhanced by the continuous confining stress provided by the inner tube. Their excellent structural performances make them particularly suitable for applications in high-rise buildings. However, if a high-rise building is damaged by fire, the economic costs associated with building repair can be high. It is very important to put the fire-damaged building back into service with the minimum post-fire repair. Thus, to predict the status of a structure under fire, its behavior should be evaluated based on the fire duration. Studies on the fire resistance of DSCT columns have been carried out for this purpose. However, they have involved the performance of the entire system without considering the effects of the DSCT column's components on the fire resistance. In this paper, the behavior of a DSCT column is investigated under an ISO-834 standard fire using an analytical method. The evaluation method for the fire resistance of a DSCT column utilizes a thermal analysis and Eurocode. In addition, the relationship between the DSCT column's components and the fire resistance is investigated, considering the confining effect. Moreover, the behavior of the DSCT column is evaluated through parametric studies of the hollow ratio, thickness of the outer tube, and thickness of the inner tube.

Keywords DSCT · Fire resistance · Confining effect · Column · ISO-834 · Inner tube

D. H. Won · T. H. Han
Coastal and Environmental Engineering Division, Korea Institute of Ocean Science and Technology, Ansan 426-744, Republic of Korea

S. Kim
Marine Research Institute, Samsung Heavy Industries Co. Ltd, 217 Munjin-ro, Daejeon 137-857, Republic of Korea

Y. J. Kang (✉)
Department of Architectural, Civil and Environmental Engineering, Korea University, 145 Anamro, Seoul 156-701, Republic of Korea
e-mail: yjkang@korea.ac.kr

Published online: 08 March 2015

1 Introduction

Columns are used in buildings and bridges. Thus, their seismic performance must be maximized to prevent any sudden collapse induced by large earthquakes. To accomplish this, the ductility in the plastic hinge regions of the columns must be increased. In general, concrete is confined by stirrups in a reinforced concrete (RC) column. A column is designed with sufficient transverse reinforcement in the form of a spiral or circular (rectangular) arrangement. Moreover, these arrangements enhance the ductility of the column to prevent the buckling of longitudinal reinforcement bars or shear failure. In a concrete-filled tubular (CFT) column, transverse reinforcement is provided by a steel tube. Compared with RC columns, CFT columns exhibit better seismic performance owing to strength enhancement via confinement by the tube. However, these can be costly when used as large substructures because of the increase in self-weight.

Moreover, the use of CFT columns for large structures has some other disadvantages. To support heavy loads, the required diameter of the column must be increased, which increases the total weight. Because of the geometric characteristics of the column, the seismic performance could consequently decrease.

The double-skinned composite tubular (DSCT) column was developed in the late 1980s [1] for the substructures of bridges and buildings. Figure 1 shows the cross section of the steel composite hollow member. Coaxial double steel tubes are arranged as shown, with the gap between them filled with concrete. The strength of a steel composite hollow member is generally 10–30 % greater than the sum of the component strengths, and a good seismic performance is obtained because of the composite effect of the interaction between the steel and concrete components [2].

The excellent structural performance of DSCT columns makes them particularly suitable for use in high-rise buildings. However, if a high-rise building is damaged by fire, the cost of building repair can be very high. It is very important to ensure that such buildings are put back into service with the minimum post-fire repair. Thus, to predict the status of a structure under fire, its behavior should be evaluated in terms of the fire duration.

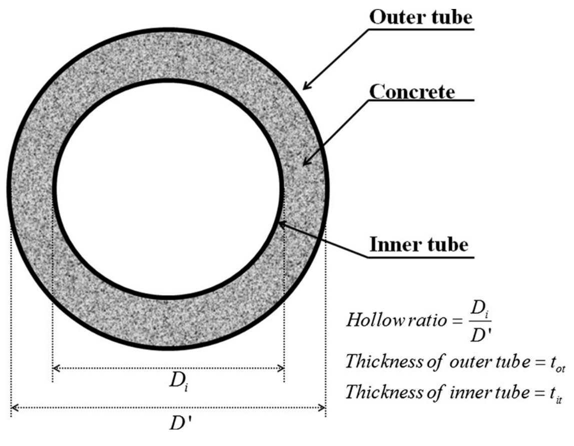

Fig. 1 Cross section of DSCT column

In addition, second-order effects occur in fire-exposed columns and should be taken care of, as they may impair the columns' fire resistance (RC columns, however, are rarely clender and buckling prone). Studies on the fire resistance of a DSCT column have been carried out for this purpose. Yang et al. [3] presented a theoretical model for the fire resistance of a DSCT column and verified it using a finite element method analysis. Han et al. [4] and Lu et al. [5–7] investigated fire resistance design methods for columns using experimental studies and finite element (FE) analyses. Park et al. [8] investigated columns in an experimental study. In addition, Pires et al. [9] and Romero et al. [10] performed experimental studies on the fire resistance of concrete-filled circular hollow columns. However, these studies investigated the performance of the entire system without considering the effects of a column's components on the fire resistance.

In this paper, the behavior of DSCT columns is analyzed under an ISO-834 [11] standard fire. An evaluation method for the fire resistance of the DSCT column is suggested using a heat transfer analysis and Eurocode [12, 13]. In addition, the relationship between the column's components and the fire resistance is investigated, considering the confining effect. The behavior of the DSCT column is also evaluated using parametric studies involving the hollow ratio, thickness of the outer tube, and thickness of the inner tube.

2 Evaluation method for fire resistance

2.1 Material properties

Because DSCT columns are made of concrete and steel tubes, it is necessary to determine their thermal and mechanical properties.

Their thermal material properties are needed to investigate the heat conduction from a fire. We use the thermal properties of steel and concrete listed in Eurocodes 2 and 3, respectively, as follows [12, 13]

The thermal properties of concrete and steel are illustrated in Figs. 2 and 3, respectively. When analyzing the specific heat of concrete, it was considered to have a moisture content of 3 % by weight. The following reference is made to the upper curve (Fig. 2b) because the temperature of concrete is raised by an increase in its conductivity.

The temperature-dependent mechanical properties are the ultimate strength, yield strength, elastic modulus, and compressive strength, as shown in Fig. 4. These are specified in Eurocodes 2 [12] and 3 [13] as follows

2.2 Heat transfer analysis and verification for application

In this paper, the heat transfer is analyzed by means of ABAQUS [14] to investigate the heat conduction in terms of the fire duration after the onset of a fire.

DC2D4, a four-node linear heat transfer element, is used to represent the steel and concrete. Furthermore, the thermal material properties for the heat transfer analysis under fire are the same as those described in the previous section.

The average furnace temperature is calculated with the information provided by the plate thermocouples.

$$T = 345 \log_{10}(8t + 1) + 20 \quad (1)$$

where T denotes the average furnace temperature in °C, and t denotes the time in minutes.

In the thermal analysis of the DSCT column in fire, appropriate boundary conditions should be introduced. The thermal force acts on the outer surface of the DSCT column. The space between the concrete

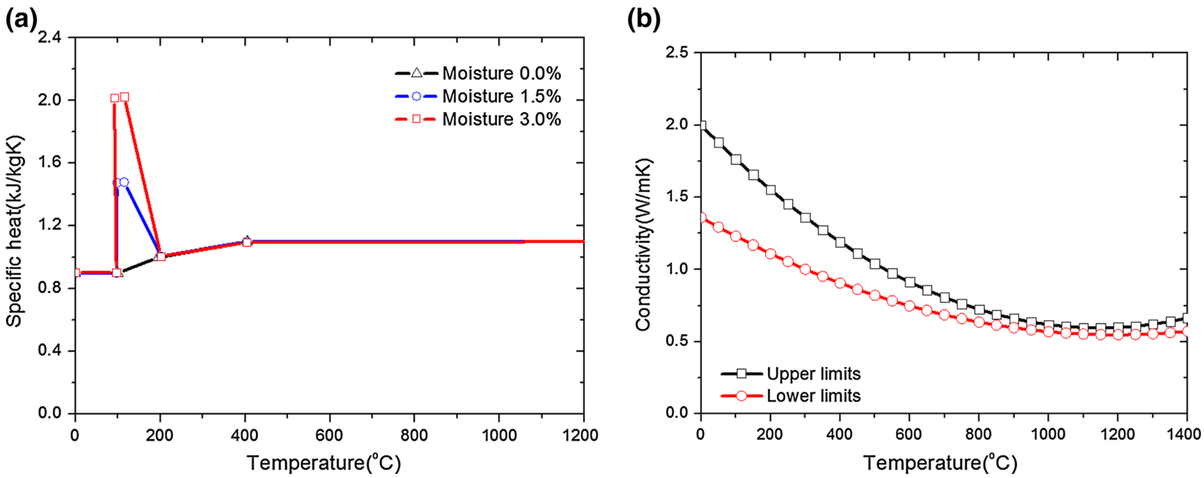

Fig. 2 Thermal properties of concrete **a** Specific heat of concrete according to Eurocode 2 [12]. **b** Conductivity of concrete according to Eurocode 2 [12]

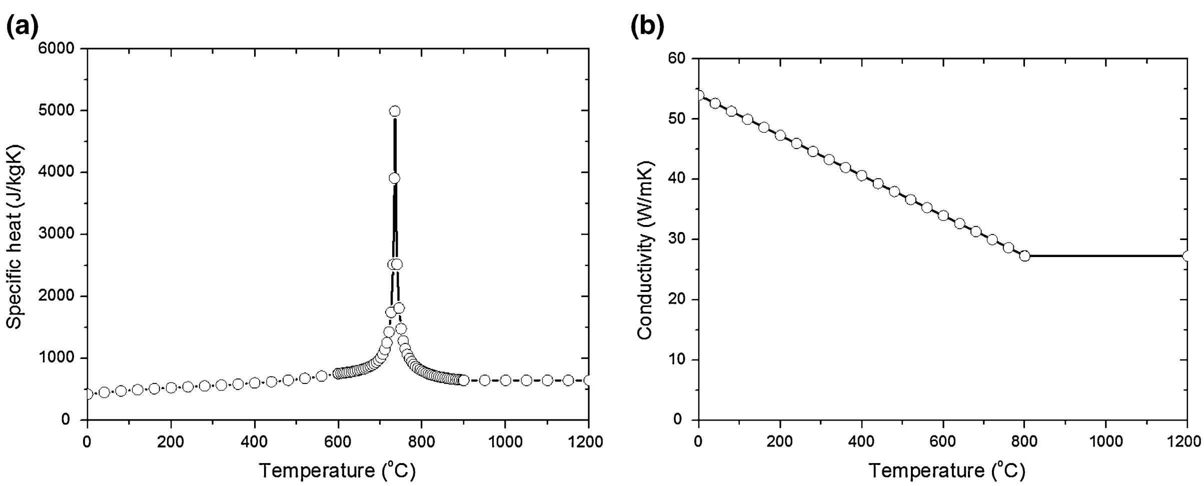

Fig. 3 Thermal properties of steel. **a** Specific heat of steel according to Eurocode 3 [13]. **b** Conductivity of steel according to Eurocode 3 [13]

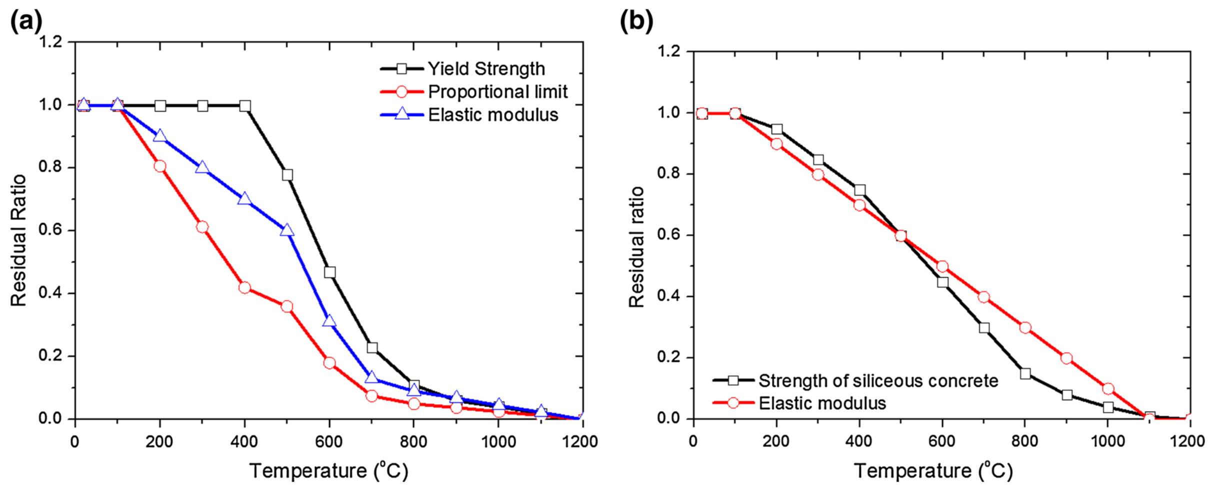

Fig. 4 Mechanical properties of steel and concrete. **a** Material properties of steel in terms of temperature in Eurocode 3 [13]. **b** Material properties of concrete in terms of temperature in Eurocode 2 [12]

Table 1 Dimensions of DSCT column for verifying analysis method [8]

Diameter of column (mm)	406.4
Thickness of outer tube (mm)	9
Thickness of inner tube (mm)	7.1
Diameter of hollow section (mm)	150

and steel tubes has a clearance of 0.01 mm, and the thermal properties of air are considered for this space.

The analysis method needs to be verified to evaluate the fire resistance of a DSCT column. In this paper, the analysis method is verified through a comparison with the results of an experimental case. The dimensions of the DSCT column, including those of the outer tube, concrete, and inner tube, are listed in Table 1. A fire test was performed under an ISO-834 standard fire by Park et al. [8].

The heat transfer analysis is performed using the suggested thermal material properties and the DSCT column dimensions listed in Table 1. Figure 5a shows the temperature distribution of the column during the fire at 30-min intervals. The heat of the fire is conducted to the hollow face from the surface of the outer tube. The analysis results and experimental results have the tolerances shown in Fig. 5b, c. In the experimental study, thermal loss occurs as a result of environmental factors. In addition, the analysis method cannot reflect the experimental conditions. For these reasons, the analysis and experimental results have errors. Figure 5b, c shows a comparison of the temperature changes at the outer surface of the concrete and inner tube, as obtained in the heat transfer analysis performed in this study. The figures indicate that as time passes, the temperatures at the outer concrete surface and surface of the inner tube gradually increase, and the tendency of this temperature increase, as obtained through a heat transfer analysis, is similar to that obtained experimentally [8]. The comparison results show that the heat transfer analysis method is reasonable; thus, it can be used for investigating the heat conduction of a fire in DSCT columns.

2.3 Confining effect of DSCT column

Han et al. [2] suggested a stress–strain model for the concrete in a DSCT column. The study reported here was performed on the basis of the following basic assumption: (1) the inner tube offers complete confining pressure unless it fails, (2) the inner tube offers no confining pressure if it fails, (3) the DSCT column fails when the outer tube fails, and (4) the concrete and tubes are not composite. The fourth assumption means the concrete is under the unconfined state if any tube fails.

Mander et al. [15] proposed a unified stress–strain approach to predict the pre-yield and post-yield behaviors of confined concrete members subjected to

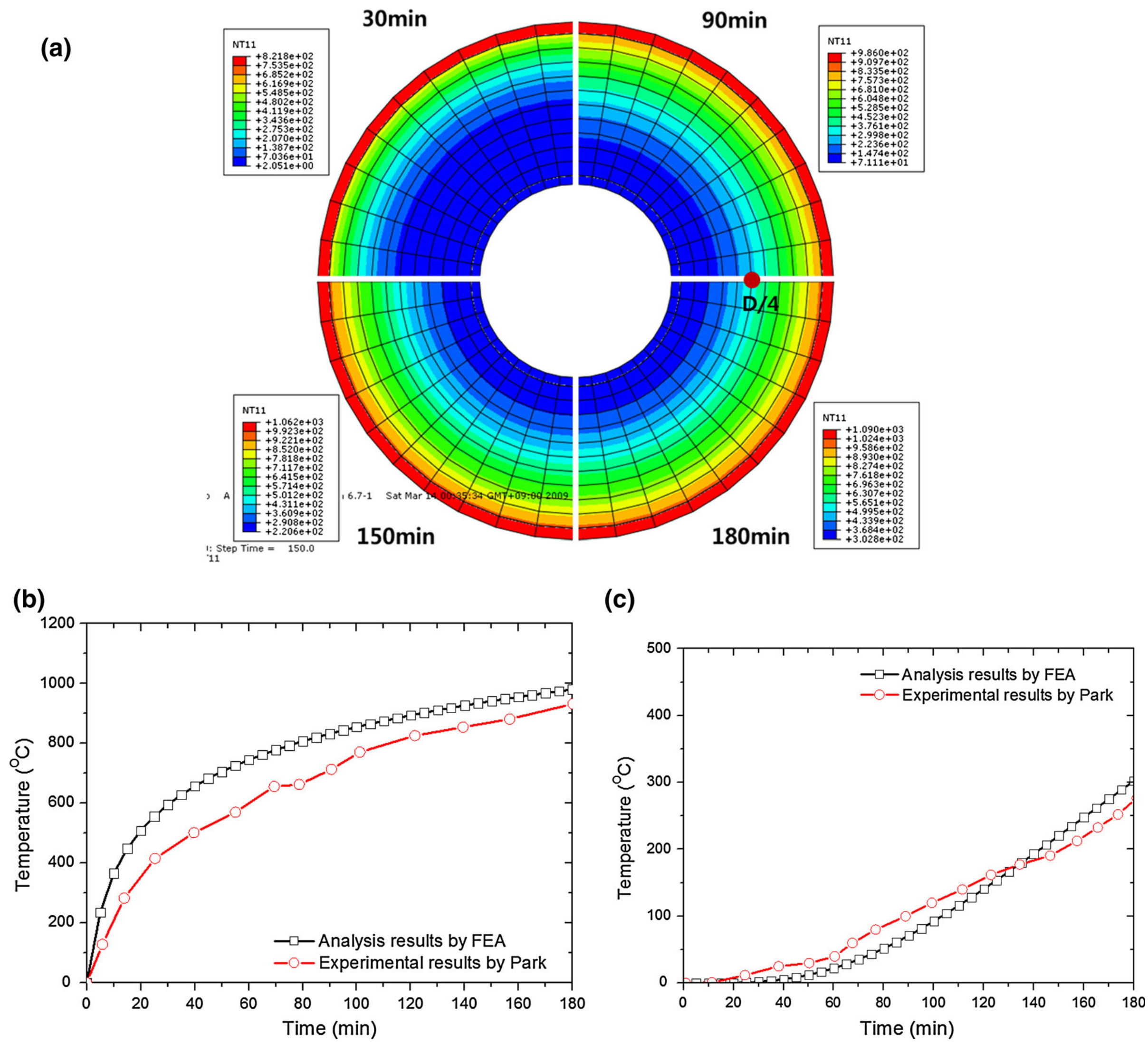

Fig. 5 Temperature distribution by heat transfer analysis. **a** Heat transfer analysis results of DSCT column. **b** Temperature on *outer* concrete face. **c** Temperature at *inner tube*

axial compressive stress. In this approach, they proposed concrete models for a monotonic compressive and tensile loading condition, a cyclic compressive and tensile loading condition, and cyclic reloading branches. One of these models is briefly reviewed to explain a new concrete model for a DSCT column. Figure 6 shows the form of the stress–strain relation in monotonic compression for confined and unconfined concrete. Mander et al. used Eq. (2), which was proposed by Popovics [16], to develop the unified stress–strain relation of confined concrete subjected to monotonic compression.

$$f_c = \frac{f'_{cc} x \cdot r}{r - 1 + x^r} \tag{2}$$

where $x = \frac{\varepsilon}{\varepsilon_{cc}}$, $r = \frac{E_c}{(E_c - E_{sec})}$, $E_{sec} = \frac{f'_{cc}}{\varepsilon_{cc}}$, f_c = the concrete stress, f'_{cc} = the confined concrete strength, ε = the uniaxial strain, ε_{cc} = the strain at the peak concrete strength, and E_c = the tangent modulus of unconfined concrete.

The tangent modulus of unconfined concrete (E_c) can be estimated to be $5000\sqrt{f'_{cc}}$ (MPa) [15]. The peak strength of confined concrete (f'_{cc}) is calculated using Eq. (3). The strain at the peak strength of unconfined

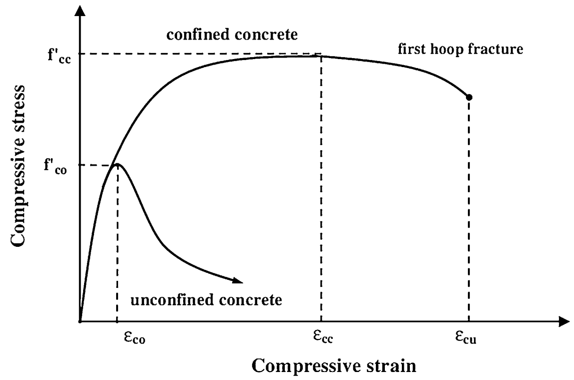

Fig. 6 Stress–strain relation of confined and unconfined concrete [2]

concrete (ε_{cc}) is given as a function of the strain at the peak strength of unconfined concrete (ε_{co}) as Eq. (4). The value of ε_{co} is usually regarded as 0.002.

$$f'_{cc} = f'_{co}\left(2.254\sqrt{1+\frac{7.94f'_l}{f'_{co}}} - \frac{2f'_l}{f'_{co}} - 1.254\right) \tag{3}$$

$$\varepsilon_{cc} = \varepsilon_{co}\left(1+5\left(\frac{f'_{cc}}{f'_{co}}-1\right)\right) \tag{4}$$

where f'_{co} = the peak strength of unconfined concrete, f'_l = the effective constant lateral confining pressure, and ε_{co} = the strain at the peak strength of unconfined concrete.

In a RC column, the spacing between the transverse reinforcements prevents them from confining the concrete core. Therefore, the effective constant confining pressure has to be used instead of the constant confining pressure (f_l). The effective constant confining pressure can be calculated by Eq. (5) using the reduction coefficient (k_e).

$$f'_l = k_e \cdot f_l \tag{5}$$

Figure 7 depicts a half section of a DSCT column under axial loading that acts only on the concrete [2]. The confining pressure is maximized when the stress acting on the outer tube (f_{ot}) reaches the yield stress (f_{oty}). From Fig. 7, the constant confining pressure (f_l) can be calculated according to Eq. (6).

$$f_l = \frac{2f_{oty}t_{ot}}{D'} \tag{6}$$

where t_{ot} denotes the thickness of the outer tube, and D' denotes the diameter of the confined concrete.

The inner and outer tubes cooperatively provide a continuous confining pressure to the concrete. Therefore, if one of the tubes fails, the concrete is in an unconfined state. Figure 7 shows a free body diagram of the half section of a DSCT column under an axial load acting only on the concrete [2]. Equations (7) and (8) can be derived from Fig. 7 respectively. The stress acting on the inner tube (f_{it}) is calculated using Eq. (9), as derived from Eq. (8).

$$f_l(D' - D_i) + 2f_{it}t_{it} = 2f_{ot}t_{ot} \tag{7}$$

$$f_lD_i = 2t_{it}f_{it} \tag{8}$$

$$f_{it} = \frac{f_lD_i}{2t_{it}} \tag{9}$$

where t_{it} denotes the thickness of the inner tube, and D_i denotes its outside diameter.

The DSCT column failures are defined under three failure modes and can be expressed using Eq. (10a, 10b, 10c), as proposed by Han et al. [2]. The first failure mode is defined as a failure of the inner tube before the outer tube yields because of buckling or yielding. The reverse condition indicates the second failure mode. In the third failure mode, both tubes fail simultaneously.

$$f_{it} > f_{lim} = smaller(f_{ity}, f_{bk})\text{: Failure Mode 1} \tag{10a}$$

Fig. 7 Confining stress on concrete in DSCT column [2]

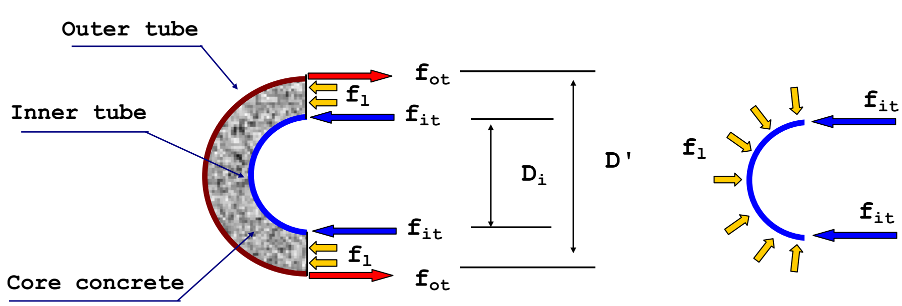

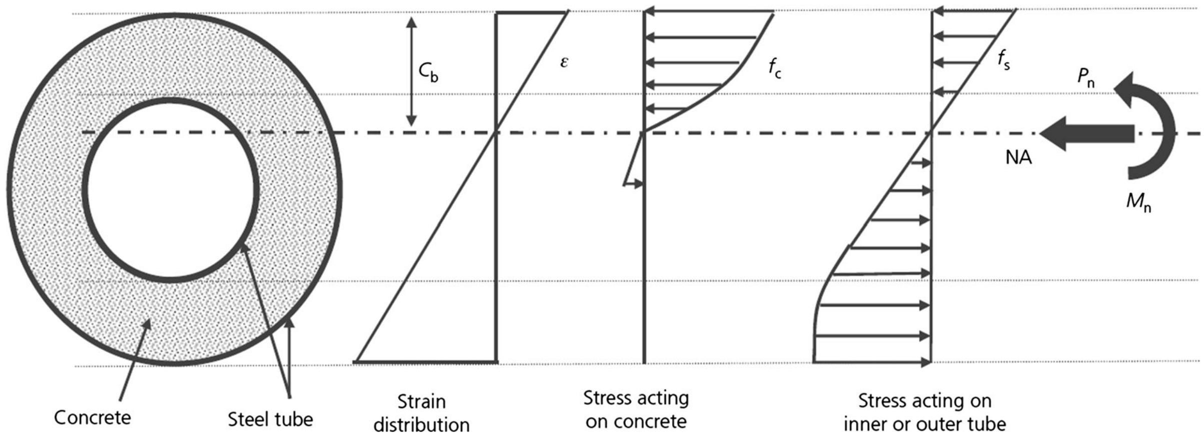

Fig. 8 Section analysis using strain compatibility and layer-by-layer approach [17]

$$f_{it} < f_{lim} = smaller(f_{ity}, f_{bk}): \text{Failure Mode 2} \quad (10b)$$

$$f_{it} = f_{lim} = smaller(f_{ity}, f_{bk}): \text{Failure Mode 3} \quad (10c)$$

where f_{ity} is the yield strength of the inner tube, f_{bk} is the buckling strength of the inner tube, and f_{lim} is the smaller value between the yield and buckling strengths of the inner tube.

The optimal performance of a DSCT column is achieved when the inner tube does not fail before the outer tube yields. The yielding failure of the inner tube determines the limit of the concrete confining pressure induced by the tube. Additionally, the buckling of the inner tube leads to the loss of the confining pressure.

2.4 Analysis of DSCT column

To describe the behavior of a DSCT column, the analytical model introduced by Han el al. [17] has been adopted for the concrete. This model is well suited for the determination of the M–N interaction envelopes. Section analyses accounting for the equilibrium, strain compatibility, and material stress–strain curves are performed by adopting a layer-by-layer technique for the numerical integration of stresses [18]. The analyses are conducted for two conditions, including (a) an unconfined concrete stress–strain curve and elasto-plastic steel behavior and (b) a confined concrete stress–strain curve and accounting for the strain hardening of the steel. Figure 8 shows the idealized section of a DSCT column. The stresses in the layers of the concrete and steel tubes are calculated as the changes in strain. The axial loads and moments for the concrete and steel tubes are found by summing them. This analysis is performed for every step by the change in the strain distribution induced by the increasing lateral load, as shown in Fig. 9. Initially, the strain distribution starts from the zero-moment condition with the strain of ε_{cc}. Then, the strain at the left side ($\varepsilon_{L,i}$) gradually decreases until the column fails. As the strain distribution changes, the distance from the neutral axis for each strain distribution ($C_{b,i}$) is given as in Eq. (11). For each stage of the strain distribution, the stresses acting on the concrete and the inner and outer tubes are calculated as in Eqs. (12)–(17). By summing them, the axial load and moment at each stage of the strain distribution are calculated as in Eqs. (18) and (19), respectively. When a constant axial load is additionally applied, the amount of strain corresponding to the constant axial load is added to the initial strain (ε_{cc}).

$$C_{b,i} = D \frac{\varepsilon_{R,i}}{\varepsilon_{R,i} - \varepsilon_{L,i}} \quad (11)$$

$$P_i^{cc} = \sum_{j=1}^{n} P_{i,j}^{CC} = \sum_{j=1}^{n} A_{i,j}^{CC} f_{i,j}^{CC} \quad (12)$$

$$P_i^{IT} = \sum_{j=1}^{n} P_{i,j}^{IT} = \sum_{j=1}^{n} A_{i,j}^{IT} f_{i,j}^{IT} \quad (13)$$

$$P_i^{OT} = \sum_{j=1}^{n} P_{i,j}^{OT} = \sum_{j=1}^{n} A_{i,j}^{OT} f_{i,j}^{OT} \quad (14)$$

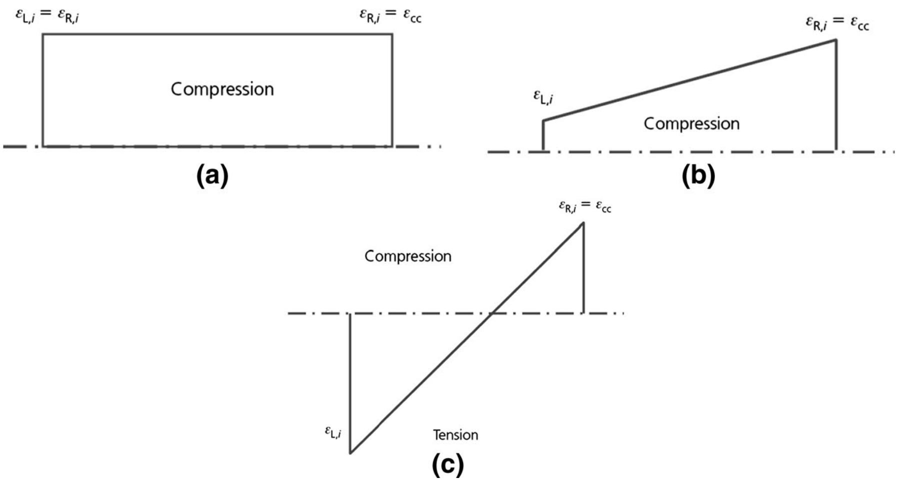

Fig. 9 Stages of strain distribution: **a** initial stage, **b** middle stage, and **c** final stage [17]

$$M_i^{CC} = \sum_{j=1}^{n} M_{i,j}^{CC} = \sum_{j=1}^{n} P_{i,j}^{CC} x_{i,j}^{CC} \quad (15)$$

$$M_i^{IT} = \sum_{j=1}^{n} M_{i,j}^{IT} = \sum_{j=1}^{n} P_{i,j}^{IT} x_{i,j}^{IT} \quad (16)$$

$$M_i^{OT} = \sum_{j=1}^{n} M_{i,j}^{OT} = \sum_{j=1}^{n} P_{i,j}^{OT} x_{i,j}^{OT} \quad (17)$$

$$P_i = P_i^{CC} + P_i^{IT} + P_i^{OT} \quad (18)$$

$$M_i = M_i^{CC} + M_i^{IT} + M_i^{OT} \quad (19)$$

The calculation procedure for the axial force-bending moment interaction to investigate the fire resistance of a DSCT column is shown in Fig. 10. After determining the material properties of the DSCT column using the heat transfer analysis and Euro-code, the material model and strain at the peak stress are calculated. The interaction between the axial force and bending moment can be calculated using the method suggested by Han et al. [17].

3 Fire resistance of DSCT column

In this section, a heat transfer analysis of a DSCT column under an ISO-834 [11] standard fire is performed using the finite element analysis method verified in the previous section. The changes in the structural properties of the DSCT column's component elements are determined based on the temperatures obtained from the heat transfer analysis. The bearing capacities under both the axial force and bending moment performances of the DSCT column in terms of the fire duration are investigated. In addition, parametric studies are performed through the selection of the main parameters, including the hollow ratio, thickness of the outer concrete, and thickness of the inner tube.

Table 2 lists the dimensions of the DSCT column used for the heat transfer analysis. The diameter of the column is 250 mm, and its hollow ratio is 0.5. The thickness of the outer tube is 4.0 mm, and the thickness of the inner tube is 2.0 mm. Here, the hollow ratio is the proportion of the inner diameter of the outer tube to the inner diameter of the concrete. The thermal material properties mentioned in Sect. 2.1 are used for the heat transfer analysis. The type of element used to represent the concrete, outer tube, and inner tube in the heat transfer analysis is DC2D4, a four–node, linear, solid element. Furthermore, an ISO-834 standard fire [11] is applied as the thermal load on the surface of the DSCT column.

Figure 11a shows the temperature distribution of the DSCT column in terms of the fire duration at 30-min intervals. The heat of the fire is conducted to the inside of the DSCT column with the fire exposure time. Here, the external boundary condition is provided by a small gap between the inner face of the external tube and the outer face of the concrete. C1, C2, and C3 denote the in terms of distance at 20.8 mm, and the internal boundary is the clearance between the inner tube and inner face of the concrete. The change

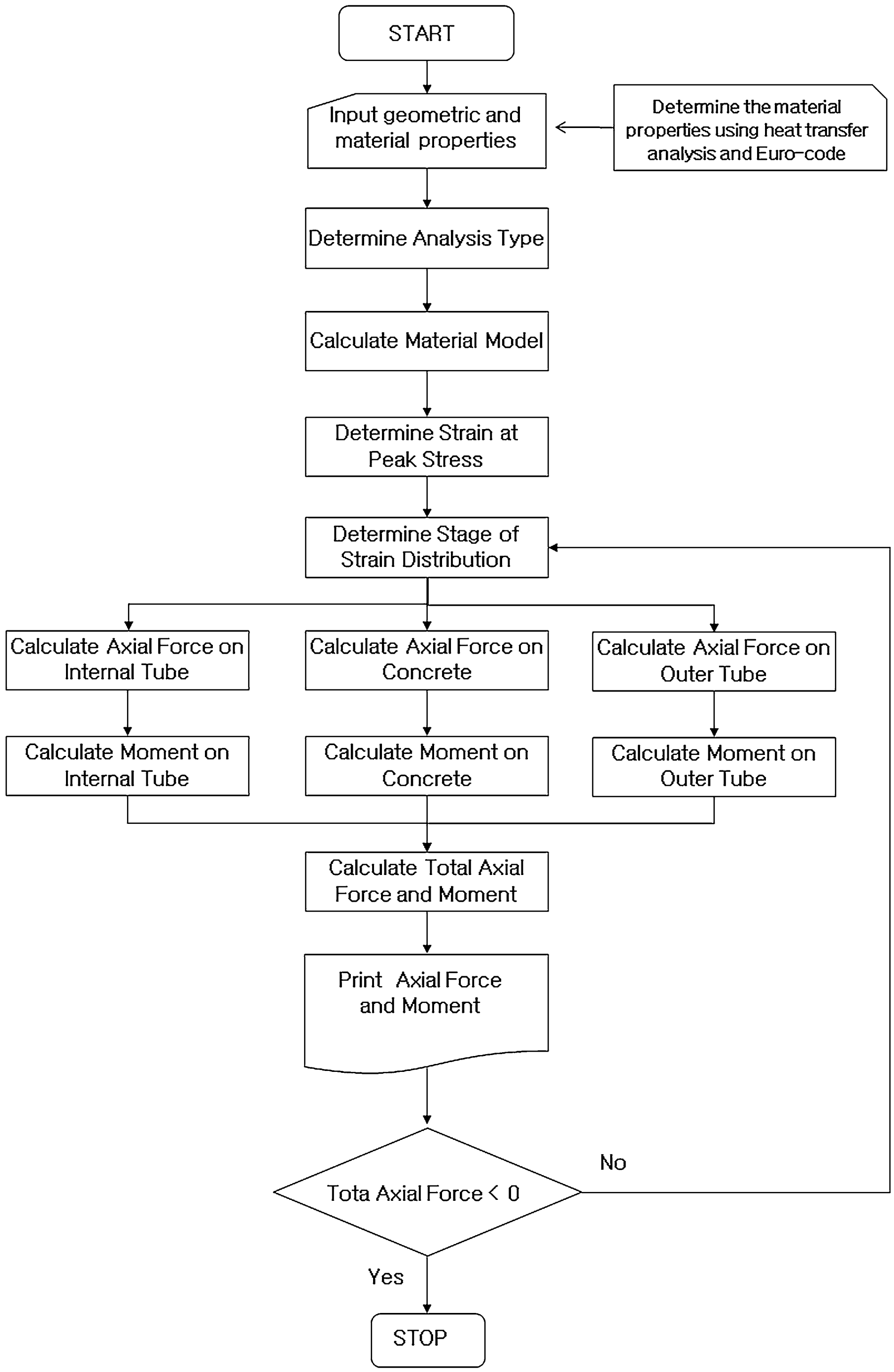

Fig. 10 Calculation procedure for axial load-bending moment interaction analyses [17]

in temperature at each location is shown in Fig. 11b. The concrete delays the heat conduction of the fire to the inside of the column because the conductivity of concrete is very low. Therefore, the temperature at the inner surface of the concrete is similar to the temperature of the inner tube, as shown in Fig. 11b.

Table 3 lists the average temperatures of the components of the DSCT column by the fire exposure

Table 2 Dimensions of DSCT column

Diameter of concrete (mm)	250.0
Yield strength of steel tube (MPa)	345.0
Elastic modulus of steel tube (MPa)	2,00,000.0
Compressive strength of concrete (MPa)	27.385
Hollow ratio	0.5
Thickness of outer tube (mm)	4.0
Thickness of inner tube (mm)	2.0
Diameter of hollow section (mm)	125.0

time. Here, the average temperature is evaluated using the temperatures calculated in all nodes. The average temperature of the outer tube reached 1028.56 °C at 120 min, whereas the concrete and inner tube reached 891.95 and 795.82 °C at 120 min, respectively.

The structural behavior of the DSCT column under the ISO-834 standard fire [11] is evaluated using the structural material properties in terms of the temperature, as shown in Fig. 4a, b. The temperature by the fire duration is based on the results of the heat transfer analysis, and the structural material properties of the DSCT column at room temperature are listed in Table 4. The compressive strength of concrete is 27.385 MPa; the yield and ultimate strengths of the steel tube are 345 and 431.25 MPa, respectively; and the elastic modulus values of the concrete and steel tube are 24,421.92 and 200,000 MPa, respectively. These are standard values.

Table 4 lists the material properties of the DSCT column components based on the fire exposure time. At close to 30 min, the average yield strength of the outer tube rapidly decreases from 345 to 34.51 MPa. Furthermore, the average ultimate strength and elastic modulus reach 34.51 and 21,000 MPa, respectively. The concrete strength is divided into those for the unconfined concrete and confined concrete. Here, the unconfined concrete strength gradually decreased from 27.38 to 2.34 MPa over the fire exposure time of 120 min. In contrast, the strength of the confined concrete rapidly decreased from 70.10 to 4.29 MPa because the outer tube failed as a result of the high temperature of the fire. Moreover, the material properties of the inner tube decrease less than those of the other components because it is located within the outer tube and concrete.

The performance of the DSCT column is evaluated by introducing the temperature dependency of the material properties, which are listed in Table 4. The P–M interaction diagram of the DSCT column, shown in Fig. 12a, is drawn at 30-min intervals. The axial and moment performances decrease as the fire exposure time passes. The residual strength, axial strength, and moment performances of the DSCT column are compared in Fig. 12b.

The axial force and pure moment performance of the DSCT column rapidly decreased 30 min after fire exposure. This shows that the performance of the DSCT column relies on that of the outer tube. The yield strength of the outer tube decreases to 10 % of its original strength, as shown in Fig. 12b. In addition, the tendencies of the axial force and pure moment

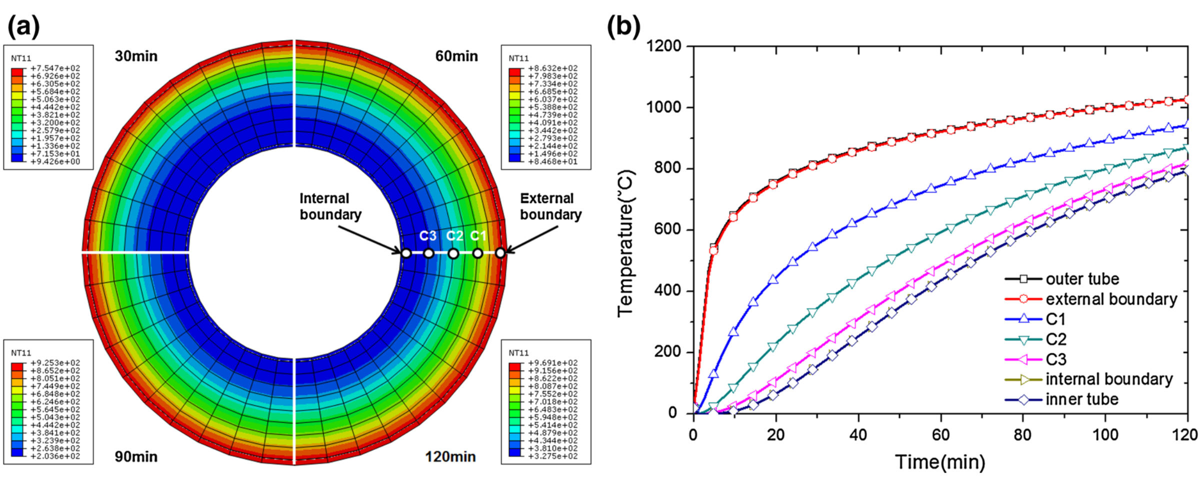

Fig. 11 Temperature distribution of DSCT column. **a** Temperature distribution of DSCT column in terms of fire duration. **b** Temperature at each location

Table 3 Average temperatures of components of DSCT column

Time (min)	Outer tube (°C)	Concrete (°C)	Inner tube (°C)
0	20.00	20.00	20.00
30	819.92	417.96	156.96
60	924.33	637.92	437.58
90	985.26	788.14	649.13
120	1028.56	891.95	795.82

Table 4 Material properties of DSCT column by fire exposure time (unit: MPa)

Time (min)	Outer tube			Concrete		Inner tube		
	Yield strength	Ultimate strength	Elastic modulus	Unconfined strength	Confined strength	Yield strength	Ultimate strength	Elastic modulus
0	345.00	431.25	2,10,000.00	27.38	70.10	345.00	431.25	2,10,000.00
30	34.51	34.51	21,000.00	19.80	26.57	345.00	431.25	1,99,500.00
60	19.02	19.02	16,800.00	10.76	14.49	316.47	316.47	1,36,500.00
90	14.81	14.81	12,600.00	4.59	7.25	121.46	121.46	52,500.00
120	11.82	11.82	10,500.00	2.34	4.29	39.67	39.67	21,000.00

performances of the confined concrete are more similar to this strength than they are to the change in the strength of the unconfined concrete. Figure 12c and d shows the performance under an eccentric aixial force (bending and axial force) by the confining effect in the DSCT column. The performance under an eccentric axial force is the result of the confining affect condition owing to the loss of outer tube strength. Likewise, the confining effect must be considered to investigate the fire-resistance of a DSCT column.

3.1 Parametric studies

In this section, the fire-resistance performance of the DSCT column is investigated through parametric studies considering the hollow ratio, thickness of the outer tube, and thickness of the inner tube. The fire resistance of the DSCT column is evaluated through parametric studies based on the suggestions in the preceding section.

3.1.1 Hollow ratio

Table 5 lists the dimensions of the analysis models in terms of the hollow ratio, i.e., the ratio of the outer and inner diameters of the confined concrete. The effect of the hollow ratio is investigated by varying it from 0.2 to 0.7, while the other dimensions of the analysis models are maintained at their original values.

Figure 13a and b shows the residual maximum moment ratio and residual maximum axial force by the confining effect in the DSCT column, respectively. The hollow ratio is changed from 0.2 to 0.7, which degrades the column performance. This behavior of the DSCT column is ascribed to the effect of the concrete. The tendency of the concrete's residual strength ratio is similar to those of the residual moment and axial force ratio, as shown in Fig. 13c. The strength of confined concrete is increased by an increase in the hollow ratio from 0.2 to 0.7. It has a large decrease rate within 30 min, after which it gradually decreases. The concrete performance is improved by increasing the thickness of the concrete wall according to the decrease in the hollow ratio. In addition, the damage to the inner tube is decreased because it obstructs the heat conduction from the fire.

3.1.2 Thickness of outer tube

The thickness of the outer tube is varied to investigate the fire resistance of the DSCT column, as summarized in Table 6. It is changed from 2.0 to 8.0 mm, while the other dimensions of the models are maintained at their original values.

Figure 14a and b shows the residual moments and axial force, respectively, of the DSCT column. The residual moment ratio and axial force ratio decrease

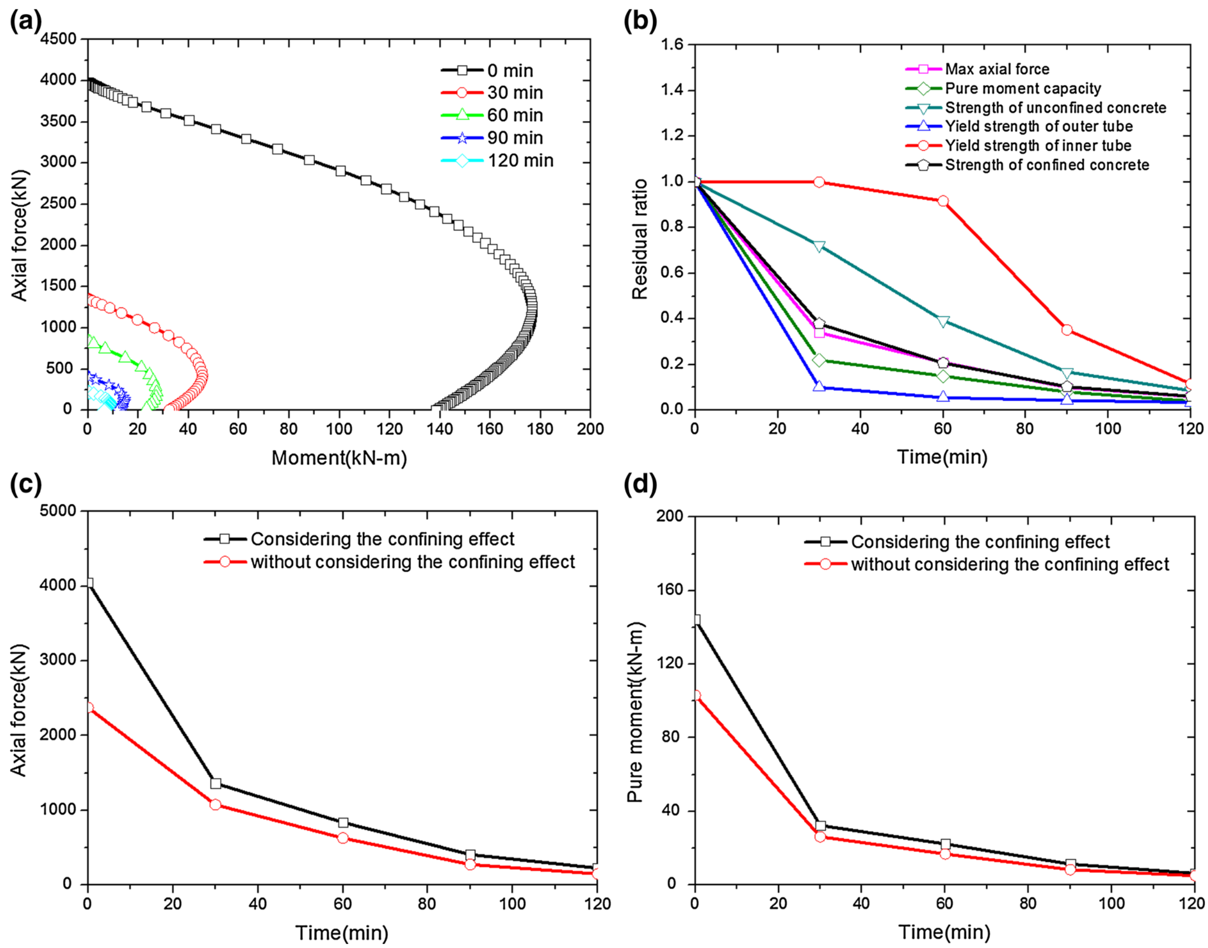

Fig. 12 Fire resistance of DSCT verification model. **a** P–M interaction diagram. **b** Residual strength ratio of components. **c** Axial force by fire exposure times. **d** Moment by fire exposure times

Table 5 Dimensions of analysis models by hollow ratio (unit: mm)

Hollow ratio	Thickness of outer tube	Thickness of inner tube	Diameter of column	Diameter of hollow section
0.2	4	2.00	250	50
0.3	4	2.00	250	75
0.4	4	2.00	250	100
0.5	4	2.00	250	125
0.6	4	2.00	250	150
0.7	4	2.00	250	175

with an increase in the thickness of the outer tube. This is because the thickness of the concrete wall is decreased by increasing the thickness of the outer tube under the same column and hollow section diameters, as listed in Table 6. The residual yield strength ratio of the outer tube is the same in all the models, and the residual yield strength ratio of the inner tube decreases with an increase in the thickness of the outer tube. This means that protecting the outer tube to guarantee the steel's tensile strength is necessary to secure the fire resistance of a DSCT column.

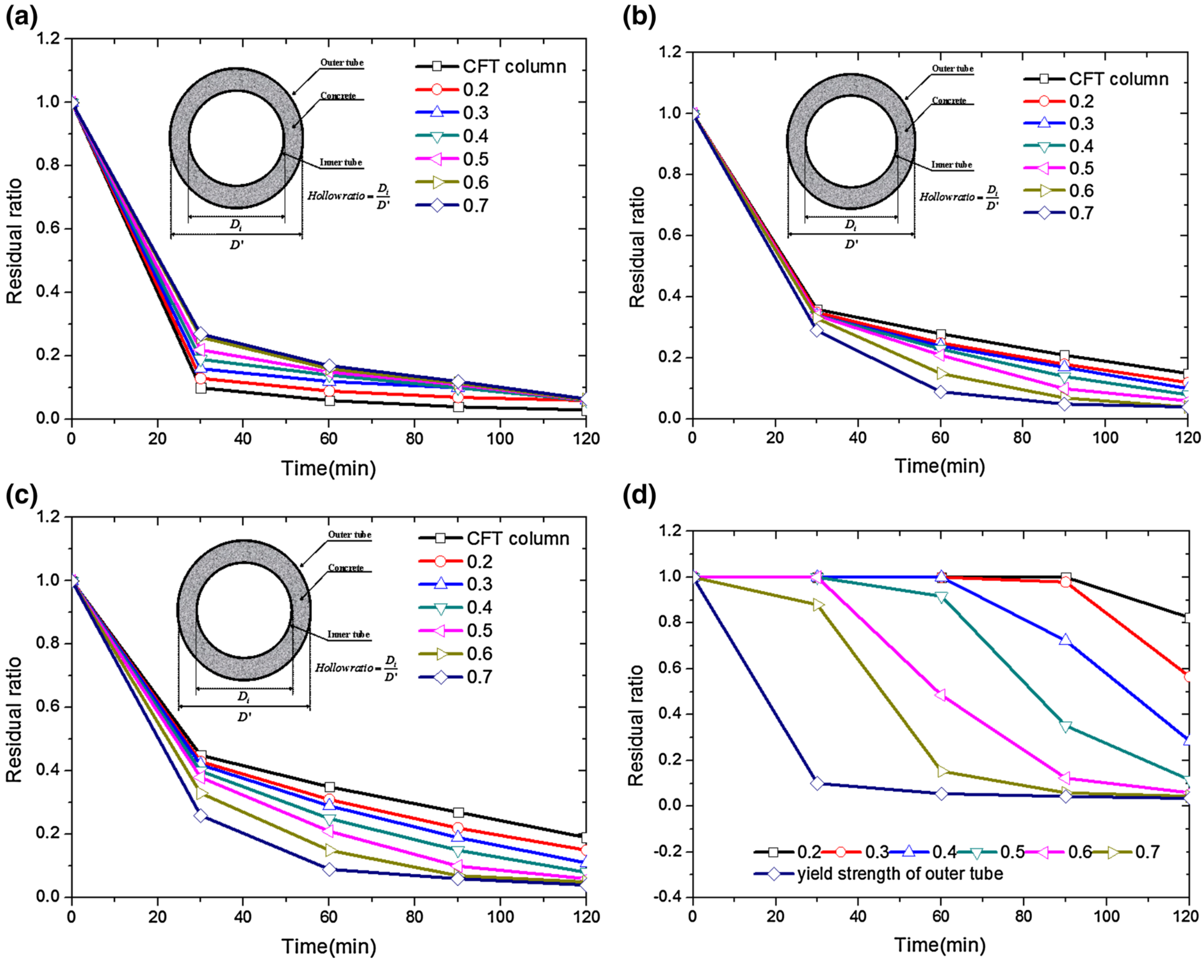

Fig. 13 Residual strength ratio of DSCT column by hollow ratio. **a** Residual pure moment ratio. **b** Residual maximum axial force ratio. **c** Residual strength ratio of confined concrete. **d** Residual yield strength ratio of *inner tube* and *outer tube*

Table 6 Dimensions of analysis models by thickness of outer tube (unit: mm)

Hollow ratio	Thickness of ou er tube	Thickness of inner tube	Diameter of column	Diameter of hollow section
0.5	2.0	4.0	250	125
0.5	2.8	4.0	250	125
0.5	4.0	4.0	250	125
0.5	5.2	4.0	250	125
0.5	6.4	4.0	250	125
0.5	8.0	4.0	250	125

3.1.3 Thickness of inner tube

Table 7 lists the dimensions of the analysis model in terms of the inner tube thickness, which is changed from 2.0 to 8.0 mm. The hollow ratio is 0.5. The thickness of the outer tube is 4.0 mm. The diameter of the column is 250 mm, and the diameter of the hollow section is 125 mm.

As shown in Fig. 15, the decreasing rate of the residual strength is reduced as the thickness of the

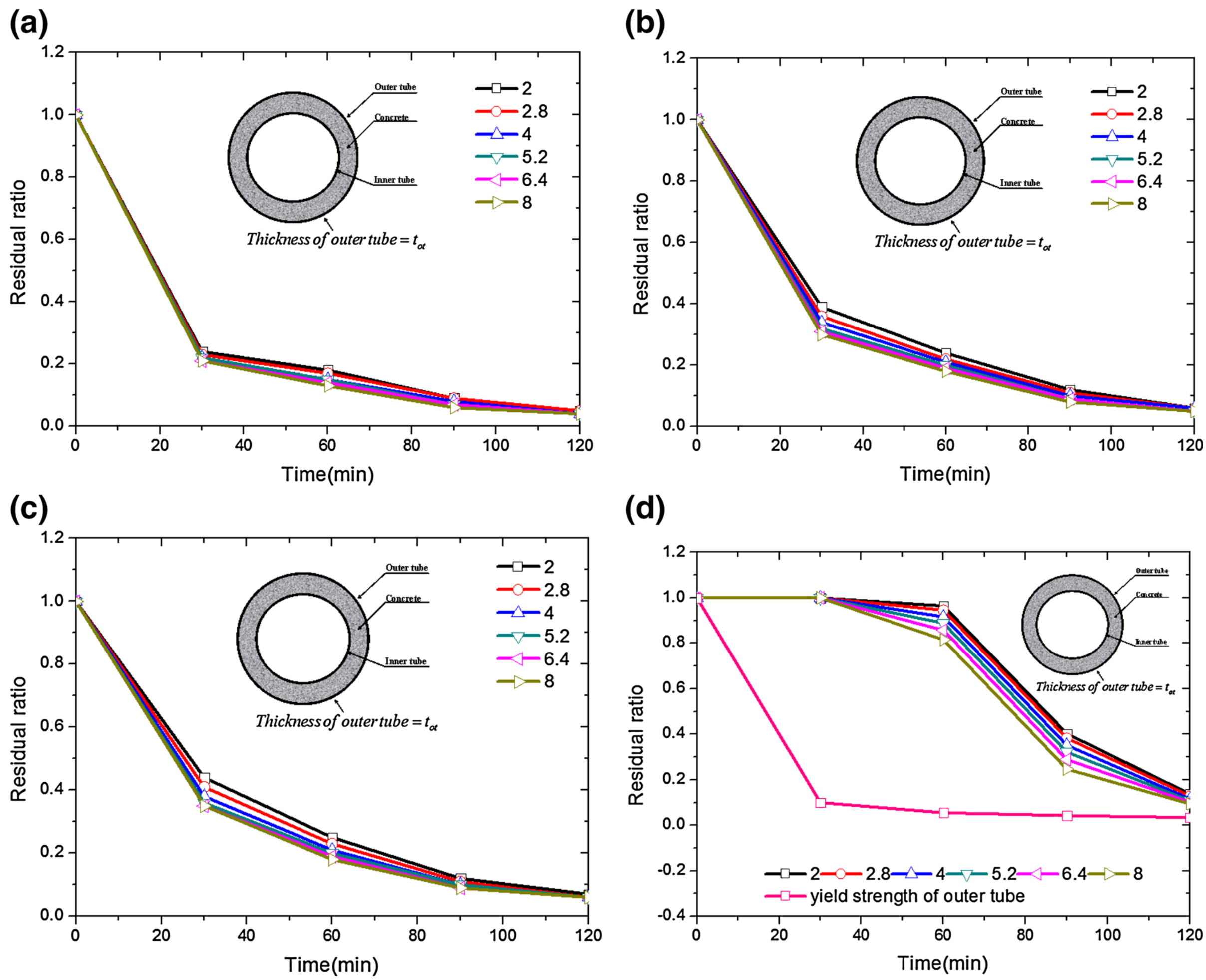

Fig. 14 Residual strength ratio of DSCT column by thickness of *outer tube*. **a** Residual pure moment ratio. **b** Residual maximum axial force ratio. **c** Residual strength ratio of confined concrete. **d** Residual yield strength ratio of *inner tube* and *outer tube*

Table 7 Dimensions of analysis models by thickness of inner tube (unit:mm)

Hollow ratio	Thickness of outer tube	Thickness of inner tube	Diameter of column	Diameter of hollow section
0.5	4.0	2.0	250	125
0.5	4.0	2.8	250	125
0.5	4.0	4.0	250	125
0.5	4.0	5.2	250	125
0.5	4.0	6.4	250	125
0.5	4.0	8.0	250	125

inner tube is increased from 2 to 8 mm. This improvement in the performance is an effect of increasing the inner tube thickness. The changes in the residual strength of the confined concrete have the same values regardless of the thickness of the outer tube. The performances of the moment and axial force are improved by increasing the thickness of the inner tube.

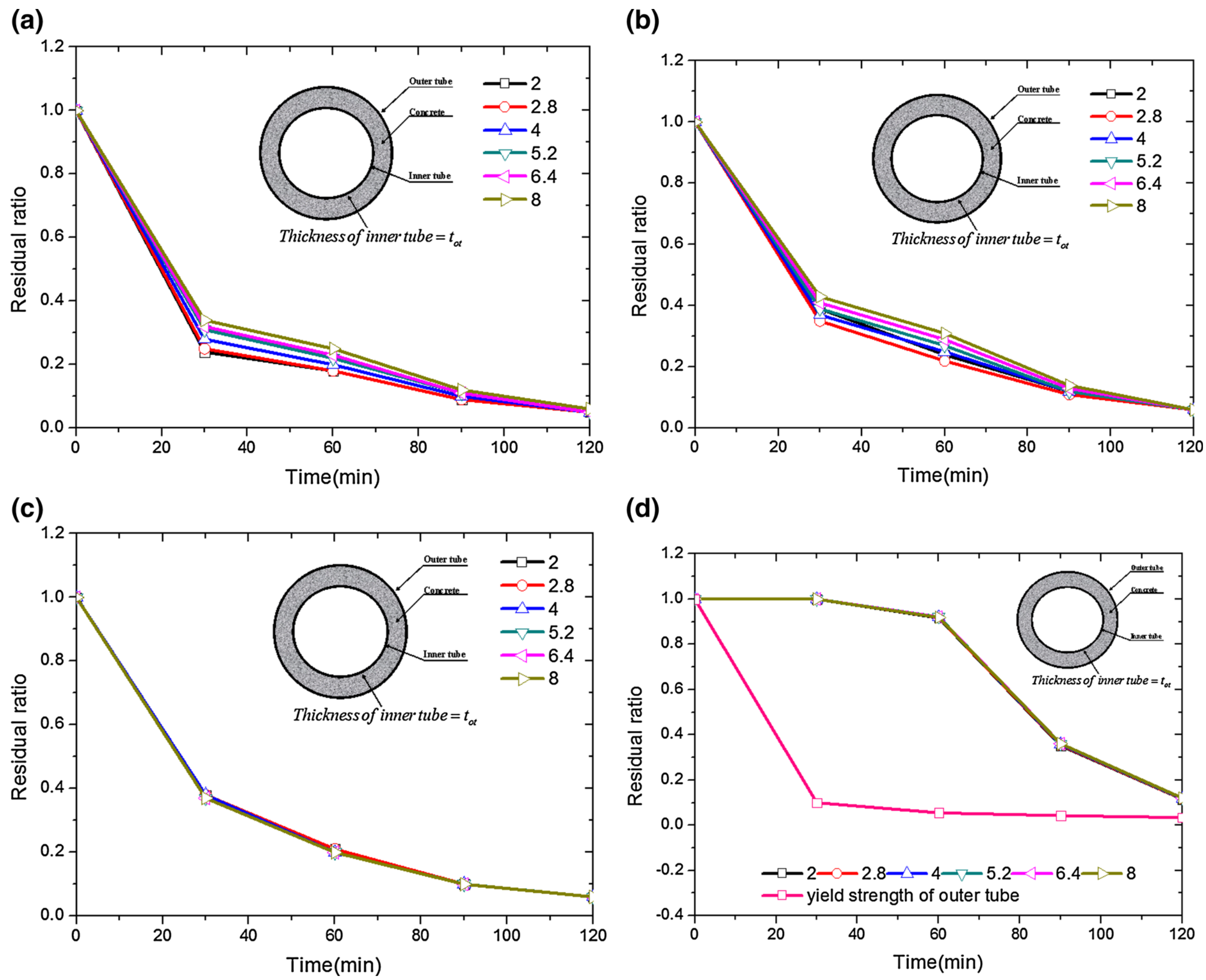

Fig. 15 Residual strength ratio of DSCT column by thickness of *inner tube*. **a** Residual pure moment ratio. **b** Residual maximum axial force ratio. **c** Residual strength ratio of confined concrete. **d** Residual yield strength ratio of *inner tube* and *outer tube*

4 Summary and conclusions

In this paper, the fire resistance of a DSCT column, considering the confining effect, was investigated using an analytical method. In addition, the effects of changing the hollow ratio, thickness of the inner tube, and thickness of the outer tube on the fire resistance were analyzed. The following conclusions were drawn.

(1) The performance under an eccentric axial force (axial force and bending moment) of the DSCT column rapidly decreased 30 min after fire exposure. This shows that the performance of the DSCT column was determined by that of the outer tube. The yield strength of the outer tube decreased to 10 % of the original strength. Moreover, the tendencies for the axial force and pure moment performances of the confined concrete were more similar than the changes in the strength of the unconfined concrete. The axial force and pure moment performances were related to the confining effect condition owing to the loss of outer tube strength. Likewise, the confining effect must be considered to investigate the fire-resistance of the DSCT column.

(2) The tendency of the concrete's residual strength ratio was similar to those of the residual moment and axial force ratio. The strength of the confined concrete was increased by an increase in the hollow ratio. It had a large decrease rate within 30 min, after which it

gradually decreased. The concrete performance was improved by increasing the thickness of the concrete wall according to a decrease in the hollow ratio. In addition, the damage to the inner tube was decreased because it obstructed the heat conduction from the fire.

(3) The residual moment ratio and axial force ratio decreased with an increase in the thickness of the outer tube. This was because the thickness of the concrete wall was decreased by increasing the thickness of the outer tube under the same column and hollow section diameters. The residual yield strength ratio of the outer tube was the same in all the models, and the residual yield strength ratio of the inner tube decreased with an increase in the thickness of the outer tube. This means that a protection method for the outer tube would be needed to secure the fire-resistance of the DSCT column.

(4) The decreasing rate of the residual strength was decreased by an increase in the thickness of the inner tube. This improvement in performance was an effect of increasing the inner tube thickness. The changes in the residual strength of the confined concrete had the same values regardless of the thickness of the outer tube. The performances of the moment and axial force were improved by increasing the thickness of the inner tube.

Acknowledgments This research was supported by a Grant (code 12 Technology Innovation E09) from the Construction Technology Innovation Program funded by the Ministry of Land, Transportation Affairs (MLTM) of the Korean government and Korea Institute of Ocean Science & Technology (KIOST), Project No. PE99321.

References

1. Shakir-Khalil H, Illouli S (1987) Composite columns of concentric steel tubes. In: Proceeding of conference on the design and construction of non conventional structures, pp 73–82
2. Han TH, Stallings JM, Kang YJ (2010) Nonlinear concrete model for double-skinned composite tubular columns. Constr Build Mater 24(12):2542–2553
3. Yang F, Han LH (2008) Concrete-filled double-skin tubular columns under fire. Mag Concr Res 60(3):211–222
4. Han LH, Zhao XL, Yang YF, Feng JB (2003) Experimental study and calculation of fire resistance of concrete-filled hollow steel columns. J Struct Eng ASCE 129(3):346–356
5. Lu H, Zhao XL, Han LH (2010) Testing of self-consolidating concrete-filled double skin tubular stub columns exposed to fire. J Constr Steel Res 66(8):1069–1080
6. Lu H, Han LH, Zhao XL (2010) Fire performance of self-consolidating concrete filled double skin steel tubular columns: experiments. Fire Saf J 45:106–115
7. Lu H, Zhao X-L, Han LH (2011) FE modelling and fire resistance design of concrete filled double skin tubular columns. J Constr Steel Res 67(11):1733–1748
8. Park SH, Song KC, Chung SK, Min BY, Choi SM (2009) An experimental study on the fire resistance of concrete-filled double skin tubular columns. The 5th international symposium on steel structures, pp 299–307
9. Pires TAC, Rodrigues JPC, Rego Silva JJ (2012) Fire resistance of concrete filled circular hollow columns with restrained thermal elongation. J Struct Steel Res 77:82–94
10. Romero ML, Espinos A, Portoles JM, Hospitaler A, Ibanez C (2014) Concrete filled circular double-tube steel columns subjected to fire. 8th International Conferences on Structures in Fire—SiF'14, Shanghai, China, pp 769–776
11. ISO 834 (1999) Fire Resistance tests—elements of building construction
12. Eurocode 2, Design of concrete structures—Part 1.2: General rules—Structural fire design
13. Eurocode 3, Design of steel structures—Part 1–2: General rules—Structural fire design, EN 1993-1-2
14. SIMULIA (2010) ABAQUS Manual 6.9.1
15. Mander JB, Priestley MJN, Park R (1984) Seismic design of bridge piers. Research report no. 84-2, University of Canterbury, New Zealand
16. Popovics S (1973) A numerical approach to the complete stress–strain curves of concrete. Cem Concr Res 3(5): 583–599
17. Han TH, Won DH, Kim SJ, Kang YJ (2013) Performance of a double-skinned composite tubular column under lateral loading: analysis. Mag Concr Res 65(2):121–135
18. Kilpatrick AE, Ranagan BV (1997) Deformation-control analysis of composite concrete columns. Research Report no. 3/97. School of Civil Engineering, Curtin University of Technology, Perth, Western Australia